www.czasopisma.pan.pl PAN POLSKA AKADEMIA NAUK www.journals.pan.pl

Arch. Metall. Mater. **65** (2020), 1, 295-304

DOI: 10.24425/amm.2020.131730

MAGDALENE EDET IKPI[1*], OKAMA EBRI OBONO[1]

CORROSION INHIBITION OF API 5L X52 CARBON STEEL BY 1-ETHYL-3-METHYLIMIDAZOLIUM-METHANESULPHONATE AND 1-ETHYL-3-METHYLIMIDAZOLIUM ACETATE IONIC LIQUIDS IN HYDROCHLORIC ACID

The corrosion inhibition behaviour of 1-Ethyl-3-methylimidazolium-methanesulphonate (EMIM[MS]) and 1-Ethyl-3-methylimidazolium acetate (EMIM[Ac]) on API 5L X-52 carbon steel in 2 M HCl was investigated using weight loss, potentiodynamic polarization and electrochemical impedance methods. The corrosion rates of carbon steel decreased in the presence of these ionic liquids. The inhibition efficiencies of the compounds increased with concentration and showed a marginal decrease with a 10°C increase in temperature. Polarization studies showed the compounds to be mixed type inhibitors with stronger anodic character. The adsorption mechanism of both compounds on the metal surface was via physical adsorption and the process obeyed the El-Awardy kinetic-thermodynamic model. The associated activation energy of corrosion and other thermodynamic parameters were calculated to elaborate on the thermodynamics and mechanism of the corrosion inhibition process. EMIM[MS] was found to inhibit the corrosion of carbon steel better than EMIM[Ac] and is attributed to the presence of the highly electronegative sulphur atom in its structure and its larger molecular size.

Keywords: Corrosion inhibition, carbon steel, ionic liquids, potentiodynamic polarization, electrochemical impedance

1. Introduction

The challenges and consequences of corrosion remains a severe and persistent problem to the metallurgical, oil and gas industry and other related industrial processes. The serious consequences of corrosion tend to jeopardize safety and health of persons and environment and inhibit technology progress because of the vital role of metals and alloys to the world economy [1]. Several approaches have been designed to protect metallic installations in industries and one of the most effective and preferred option involves the use of inhibitors [2-4]. It has been established that the initial mechanism in any corrosion inhibition process is the adsorption of the inhibitor on the surface of the metal. The adsorption of the inhibitor blocks the active centers for corrosion and protects the metal. Ionic liquids (ILs) are emerging as smart and excellent solvents, which are made of positive and negative ions that pack so poorly together that they are liquids near room temperature [5,6]. They offer significant properties which make them potentially attractive alternatives for volatile organic solvents. These include a negligible vapour pressure, high thermal stability, non-flammability, decent solubility for organic, inorganic and organometallic compounds, non-coordinating but good solvating ability, high ionic conductivity, and an electrochemical potential window [7-11]. The molecular structure is capable of forming micelles and lowering interfacial tension of aggressive media, which leads to an improvement in surface wetting and adsorption [12]. These properties have a beneficial effect on exposed surfaces and may be responsible for the corrosion inhibition of metals. As ILs present a molecular structure suitable to be readily adsorbed on the metallic surface [13], they may constitute a larger potential group to be researched as corrosion inhibitors.

Recently, imidazolium compounds and several other organic compounds containing heteroatoms like N, S, O, P and π-bonds have been reported to show corrosion resistant behaviour on copper [14], steel [15-18] and aluminium [19,20]. It was discovered that the action of such inhibitors depended also on the specific interaction between the functional groups and the metal surface. This study therefore seeks to establish the effect of molecular structure and size of two ionic liquids; 1-Ethyl-3-methylimidazolium acetate and 1-Ethyl-3-Methylimidazolium-methanesulphonate on the kinetics of the corrosion reaction of API 5L X52 carbon steel in 2 M HCl using gravimetric and electrochemical assessment techniques as well as appraise the mechanism of adsorption and thermodynamic considerations of the corrosion inhibition process.

[1] CORROSION AND ELECTROCHEMISTRY RESEARCH LABORATORY, DEPARTMENT OF PURE AND APPLIED CHEMISTRY, UNIVERSITY OF CALABAR, CALABAR-NIGERIA

* Corresponding author: meikpi@unical.edu.ng, me_ikpi@yahoo.com

© 2020. The Author(s). This is an open-access article distributed under the terms of the Creative Commons Attribution-NonCommercial License (CC BY-NC 4.0, https://creativecommons.org/licenses/by-nc/4.0/deed.en which permits the use, redistribution of the material in any medium or format, transforming and building upon the material, provided that the article is properly cited, the use is noncommercial, and no modifications or adaptations are made.

2. Experimental

2.1. Materials

API 5L X52 carbon steel cut from its parent pipe was used as the test material for these experiments and has the chemical composition shown in Table 1. Samples were obtained from pipeline and product marketing company (PPMC) Port Harcourt, Nigeria. The preparation of the specimen for experimental measurement is as reported by Ikpi and Abeng [21]. 2 M HCl solution was prepared by dilution of an analytical reagent grade 37% HCl with distilled water. The inhibitor compounds used were 1-Ethyl-3-methylimidazolium acetate EMIM[Ac] and 1-Ethyl-3-Methylimidazolium-methanesulphonate EMIM[MS]. EMIM[MS] is a colorless organic compound with molecular formula $C_7H_{14}N_2O_3S$ and density 1.247 g/cm^3 (Fig. 1a) whereas EMIM[Ac] is an organic compound with molecular formula- $C_8H_{14}N_2O_2$ and density 1.027 g/cm^3 at 25°C (Fig. 1b).

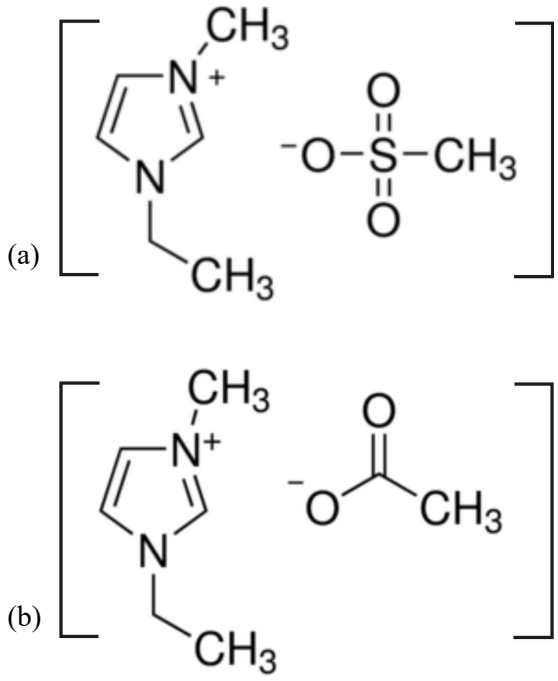

Fig. 1. Structural formula of (a) 1-Ethyl-3-Methylimidazolium-methansulfonate (EMIM[MS]) and (b) 1-Ethyl-3-methylimidazolium acetate (EMIM[Ac])

EMIM[MS] with molecular weight 206.26 g mol^{-1} and EMIM[Ac] with molecular weight 170.21 g mol^{-1} both of ≥95% purity were obtained from Sigma Aldrich, Germany. A stock solution of 0.01 M of each inhibitor was prepared with 2 M HCl solution. From this stock solution, test solutions of different concentrations (0.001 M, 0.005 M, and 0.01 M) of the inhibitors were prepared by dilution.

2.2. Weight loss measurements

200 ml of 2 M HCl in the absence and presence of different concentrations of EMIM[MS] and EMIM[Ac] inhibitors were placed in beakers. Finely abraded and dried carbon steel coupons with dimensions (1×1×1) cm^3 were weighed (DENVER instrument) and singly suspended into the beakers at room temperature with the help of a polymeric string. The experiment was allowed to run for a period of 20 days (480 hrs). The first set of coupons were retrieved after 24 hrs. Subsequently, other sets of coupons were retrieved after 5, 10, 15 and 20 days of unperturbed immersion. The retrieved coupons were rinsed in ethanol, cleaned by mild scrubbing with a bristle brush to remove all the corrosion products and then dried in acetone and reweighed. The weight loss W_L (mg) was evaluated as the difference in weight of the coupons before and after the test. A plot of W_L per unit area against time allowed for the determination of the corrosion rate (mg cm^{-2} hr^{-1}) from the slope (W_L/At). The corrosion rate CR in units of mm y^{-1}, the degree of surface coverage θ and the inhibition efficiency IE (percentage of the surface coverage) were calculated as follows in Eq. (1), (2) and (3) respectively;

$$CR = \frac{87.6W_L}{\rho At} \tag{1}$$

$$\theta = \left(\frac{CR_{(blank)} - CR_{(inh)}}{CR_{(blank)}} \right) \tag{2}$$

$$IE = \left(\frac{CR_{(blank)} - CR_{(inh)}}{CR_{(blank)}} \right) \times 100 \tag{3}$$

where ρ is the density of Fe in g cm^{-3}, A is the exposed surface area in cm^2, t is the time of exposure in hrs and $CR_{(blank)}$ and $CR_{(inh)}$ are the corrosion rates in the uninhibited and inhibited solutions respectively.

2.3. Electrochemical measurements

Experiments were undertaken in 2 M HCl solutions in the absence and presence of different concentrations of EMIM[MS] and EMIM[Ac] (0.001 M, 0.005 M, 0.01 M) using a conventional three-electrode cell assembly with a Pt plate counter electrode, a saturated calomel electrode (SCE) as reference electrode and the sample with a 1 cm^2 exposed surface area as the working electrode. The sample was immersed for 30 minutes prior to each measurement to attain a steady state. Potentiodynamic

TABLE 1

Elemental composition of API 5L X52 carbon steel

Element	C	Mn	Si	P	S	Cr	Ni	Ti	Nb	Mo	V	Al
Composition	0.22	1.40	0.45	0.025	0.015	0.20	0.20	0.04	0.15	0.08	0.15	0.030

polarization measurements were conducted at 303 K and 313 K, while impedance measurements were carried out at 303 K. The temperature was maintained by placing the cell in a thermostat water bath. Electrochemical measurements were made using a GAMRY Reference 600 potentiostat connected to a computer and controlled with Gamry Framework software to record data and Echem Analyst software for analysis of the polarization and impedance curves. The electrode potential varied from -250 mV/SCE with respect to the open circuit potential (OCP) to 700 mV/SCE above OCP with scanning rate of 0.5 mV s^{-1} for potentiodynamic current-polarization curves. EIS measurements were carried out over the frequency range of 10^5 to 5×10^{-2} Hz, with a signal amplitude perturbation of 10 mV. The corrosion rate CR (mm y^{-1}) was computed using Eq. (4);

$$CR = \frac{I_{corr}\, k\,(EW)}{\rho A} \tag{4}$$

where I_{corr} is the corrosion current density, k a constant (3272 mm A^{-1} cm^{-1} y^{-1}), EW the equivalent weight (g equivalent^{-1}), ρ the density of Fe (g cm^{-3}) and A the exposed surface area (cm^2). From potentiodynamic polarization measurements, IE was calculated from values of I_{corr} using Eq. (5);

$$IE = \left(\frac{I_{corr(blank)} - I_{corr(inh)}}{I_{corr(blank)}}\right)\times 100 \tag{5}$$

where $I_{corr(blank)}$ and $I_{corr(inh)}$ are the uninhibited and inhibited corrosion current densities, respectively.

From electrochemical impedance measurements, IE was calculated from charge transfer resistance (R_{ct}) values using Eq. (6);

$$IE = \left(\frac{R_{ct(inh)} - R_{ct(blank)}}{R_{ct(inh)}}\right)\times 100 \tag{6}$$

where, $R_{ct(inh)}$ and $R_{ct(blank)}$ are the inhibited and uninhibited charge transfer resistance, respectively.

3. Results and discussion

3.1. Weight loss

Fig. 2a and 2b show the variation of W_L per unit area with time for the corrosion of carbon steel in 2 M HCl containing various concentrations of EMIM[MS] and EMIM[Ac] respectively. The plots reveal that the weight loss of carbon steel in the absence of these compounds (blank) is higher than those obtained for solutions containing various concentrations of the imidazolium-based ILs. This indicates that the ILs retarded and inhibited the corrosion of carbon steel in HCl solutions. The plots also reveal that the weight loss of carbon steel decreases with increase in the concentration of the inhibitor, indicating that the inhibition potentials of EMIM[MS] and EMIM[Ac] increase with increasing concentration.

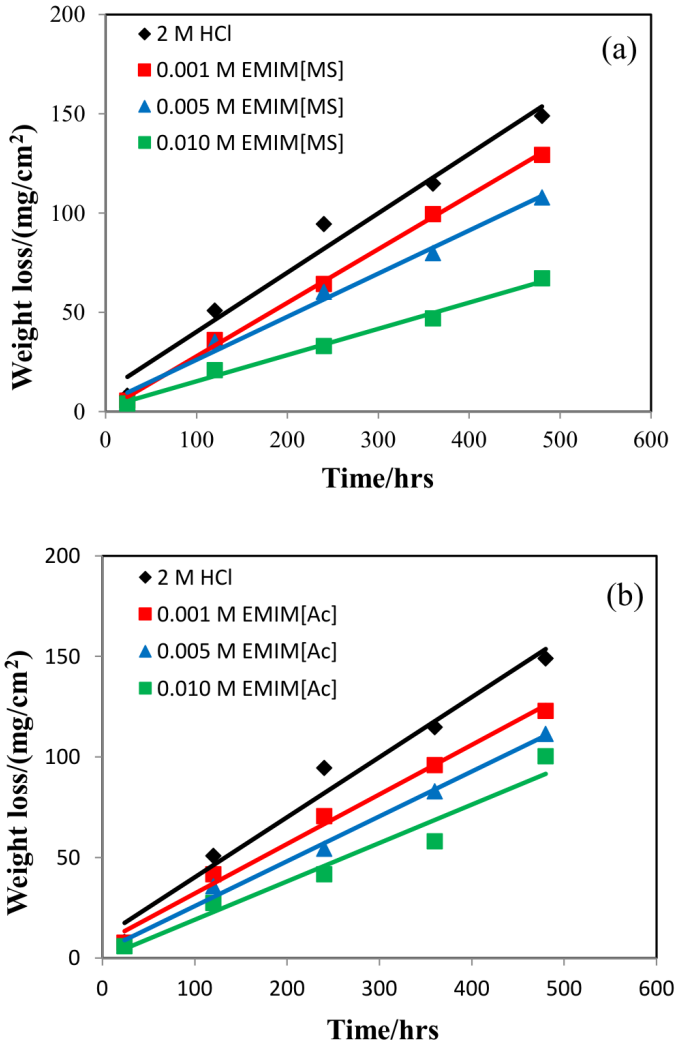

Fig. 2. Variation of weight loss (mg/cm^2) with time (hrs) for the corrosion of carbon steel in 2 M HCl containing various concentrations of (a) EMIM[MS] and (b) EMIM[Ac]

Table 2 presents calculated values of weight loss, corrosion rate, surface coverage and inhibition efficiency after immersion times of 24 hrs, 120 hrs, 240 hrs, 360 hrs and 480 hrs at 303 K in 2 M HCl in the absence and presence of various concentrations of inhibitors. The slopes (W_L/At) of the curves of Fig. 2a and 2b averages the rate of corrosion and are shown in Table 2. The R^2 value shows a closeness to unity indicating that the data approximates to the fitted line and that the rate of corrosion can be described as uniform in the 20 days period of immersion. The corrosion inhibition efficiency of both inhibitor compounds increases with inhibitor concentration. The corrosion rate decreased considerably with an increase in concentration of both inhibitors. The increase in efficiency of inhibition with concentration of inhibitors indicates that the inhibitors are adsorption inhibitors. It also indicates that more inhibitor molecules are adsorbed on the metal surface at higher concentration leading to greater surface coverage [22]. Molecular orientation and availability of electrophilic adsorption sites of the inhibitors are possible factors responsible for effectiveness of both inhibitors and which is in the order EMIM[MS] > EMIM[Ac].

TABLE 2

Calculated values of weight loss per unit area, corrosion rate, surface coverage and inhibition efficiency after different immersion times at 303 K in 2 M HCl in the absence and presence of EMIM[MS] and EMIM[Ac]

Inhibitor system	Inhibitor conc. (M)	W_L per unit area at different immersion times (mg cm^{-2})					W_L/At (mg cm^{-2} hr^{-1})	R^2	CR (mm y^{-1})	θ	IE (%)
		24 hrs	120 hrs	240 hrs	360 hrs	480 hrs					
Blank	0	8.00	50.83	94.50	114.83	149.00	0.2987	0.975	3.321		
EMIM[MS]	0.001	5.50	36.00	64.33	99.50	129.33	0.2698	0.998	2.999	0.10	10
	0.005	4.50	35.17	60.33	79.83	107.83	0.2173	0.989	2.416	0.27	27
	0.010	4.00	20.83	33.00	47.00	67.17	0.1322	0.991	1.470	0.56	56
EMIM[Ac]	0.001	7.67	41.67	70.67	96.00	123.00	0.2464	0.990	2.739	0.18	18
	0.005	5.50	35.67	54.33	83.00	111.50	0.2232	0.993	2.481	0.25	25
	0.010	5.83	27.50	41.67	58.17	100.33	0.1909	0.955	2.122	0.36	36

3.2. Potentiodynamic polarization measurements

The potentiodynamic polarization curves for carbon steel in 2 M HCl solution with different concentrations of inhibitors at 303 K and 313 K are shown in Fig. 3. The polarization parameters of corrosion current density (I_{corr}), corrosion potential (E_{corr}), corrosion rate (R_{corr}) and anodic and cathodic Tafel constants (β_a and β_c respectively) for both ILs as obtained from the Tafel fit using Gamry Echem analyst software are given in Table 3. It could be observed that the addition of the ILs caused a positive shift in E_{corr} especially at high concentrations. It has been reported that a compound can be classified as an anodic and cathodic type inhibitor on the basis of shift in E_{corr} value [23]. The report states that if displacement of E_{corr} value is greater than 85 mV, towards anode or cathode with reference to the blank, then an inhibitor is categorized as either anodic or

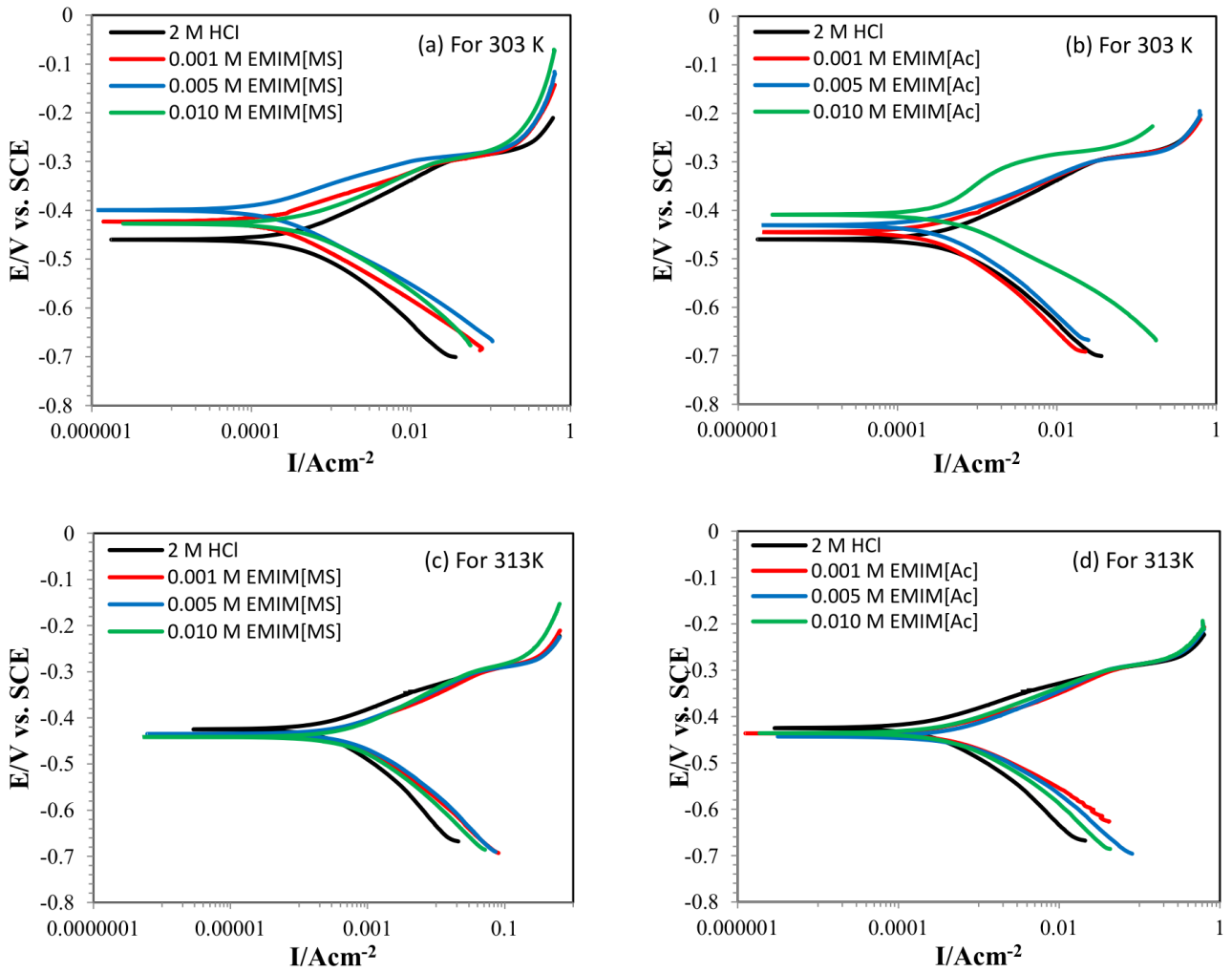

Fig. 3. Potentiodynamic polarization curves for API 5L X52 carbon steel in 2 M HCl solution containing various concentrations of (a) EMIM[MS] and (b) EMIM[Ac] both at 303 K and (c) EMIM[MS] and (d) EMIM[Ac] both at 313 K

TABLE 3

Data obtained from potentiodynamic polarization measurements carried out in the absence and presence of EMIM[MS] and EMIM[Ac] at 303 K and 313 K

Inhibitor system	Inhibitor conc. (M)	Temp. (K)	$-E_{corr}$ (mV)	i_{corr} (μA cm^{-2})	β_a (mV dec^{-1})	β_c (mV dec^{-1})	R_{corr} (mm y^{-1})	θ	IE (%)
Blank	0	303	460	349	83.7	90.6	4.046		
EMIM[MS]	0.001		423	250	79.1	111.4	2.899	0.28	28
	0.005		400	200	85.3	90.4	2.319	0.43	43
	0.010		424	155	54.2	65.8	1.797	0.56	56
EMIM[Ac]	0.001		445	289	72.8	116.9	3.351	0.17	17
	0.005		431	269	62.8	92.2	3.119	0.23	23
	0.010		409	220	94.9	39.1	2.551	0.37	37
Blank	0	313	425	386	107.4	138.5	4.475		
EMIM[MS]	0.001		436	320	56.8	74.6	3.710	0.17	17
	0.005		435	254	59.6	58.0	2.945	0.34	34
	0.010		433	182	58.2	60.3	2.110	0.53	53
EMIM[Ac]	0.001		445	334	88.7	127.6	3.872	0.13	13
	0.005		443	308	66.2	43.8	3.571	0.20	20
	0.010		436	260	61.8	71.4	3.014	0.33	33

cathodic, otherwise, inhibitor is treated as a mixed type inhibitor In this study, maximum displacement of E_{corr} value was around 60 mV, indicating that both anodic and cathodic reactions are affected by the addition of both inhibitors. In addition, β_c and β_a changed with respect to inhibitor concentration. This suggests that the inhibitors are mixed type with more anodic character. The inhibition effect can be said to be due to active sites-blocking effect since different corrosion potentials are exhibited in the inhibitor-containing solution and in solutions without inhibitor [24]. At 303 K, the anodic slopes shifted towards lower current densities relative to the reference sample on introduction of the compounds whereas the cathodic slopes shifted towards higher current densities. The decrease in the corrosion rates recorded in the presence of both inhibitors, which indicates decreased metal dissolution is suggestive of a suppression of corrosion at anodic sites and greater cumulative effect of anodic current densities on the total corrosion current density. *IE* results obtained show values increasing in the case of both inhibitors used when the concentration of the inhibitors are increased. This indicates adsorption of inhibitor on the metal surface and the process improving with increasing inhibitor concentration. The effectiveness of the two inhibitors are in the order EMIM[MS] > EMIM[Ac], which is in good agreement with results obtained from weight loss measurement. The corrosion rate and inhibition efficiency values obtained from weight loss and potentiodynamic polarization measurements for both inhibitors appears somewhat comparable and with greater agreement in the inhibition efficiency values.

A look at the polarization plots for the corrosion of carbon steel in 2 M HCl, containing various concentrations of EMIM[MS] (Fig. 3a and 3c) and EMIM[Ac] (Fig. 3b and 3d) at 303 K and 313 K respectively, shows clearly very little displacement of E_{corr} values at 313 K with reference to the blank and no marked deflections in the anodic curves compared to those at 303 K for the concentration of inhibitors studied. I_{corr} values increased slightly with a temperature increase of 10°C in the uninhibited and inhibited solutions (Table 3), reflecting a marginal decrease in the inhibition efficiencies for the inhibitors at the concentrations studied. Increase in temperature leads to an acceleration of all processes involved in corrosion: electrochemical, chemical, transport, etc. [25]. A decreasing inhibition efficiency with temperature is interpreted on the basis that the increase in temperature results in desorption of the inhibitors from the steel surface suggesting a physisorption type mechanism of the organic molecules on the surface of the metal.

3.3. Impedance measurements

Nyquist plots for the corrosion of carbon steel in the absence and presence of different concentrations of EMIM[MS] and EMIM[Ac] are presented in Fig. 4. The Nyquist plots are characterized by slightly depressed capacitive semicircles whose diameter increases with inhibitor concentration indicating that the corrosion process is mainly controlled by charge transfer. The charge transfer resistance represents the dissolution of iron since iron is the major component of the steel sample and the fact that iron is a highly active metal in acidic media [26]. The electrochemical processes taking place at the steel surface can be understood by fitting the impedance data into an equivalent circuit model (Fig. 5). The values of the circuit components are shown in Table 4. The model has a component of resistance from the solution R_s, a film resistance R_f arising from a protective layer of inhibitor molecules covering the steel surface and a charge transfer resistance R_{ct} on account of the dissolution of iron. It also has constant phase elements (CPE) Q_f and Q_{dl} associated with the protective film and the double layer on the steel surface respectively. The charge transfer resistance can likewise be obtained from the diameter of the capacitive semicircles in the Nyquist plots and is referred as R'_{ct} in Table 4.

The film resistance and the charge transfer resistance increases as the concentration of the inhibitor molecules

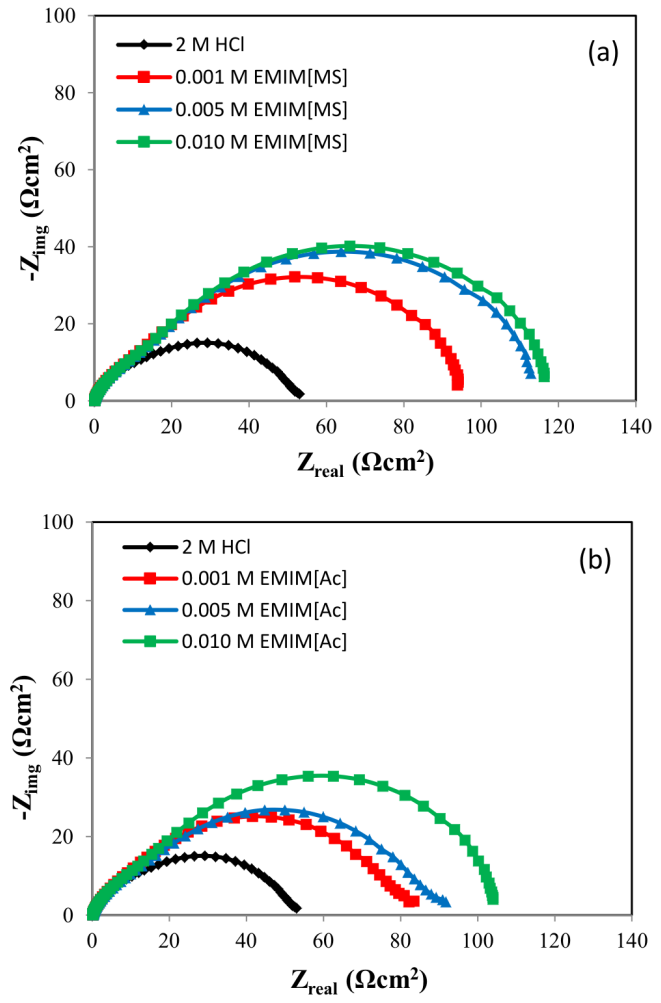

Fig. 4. Nyquists plots in the absence and presence of different concentrations of (a) EMIM[MS] and (b) EMIM[Ac] at 303 K

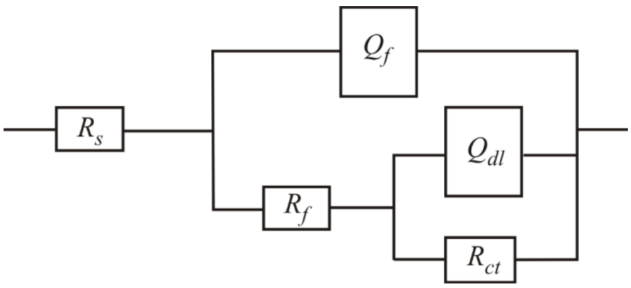

Fig. 5. Equivalent circuit model used to fit the impedance data

increases. The values of R_f for EMIM[MS] are greater than those for EMIM[Ac]. The higher resistance experienced for the EMIM[MS] infers a better protection of the adsorbed film of EMIM[MS] molecules. It is also observed that R_{ct} for EMIM[MS] molecules is slightly higher than the values obtained for EMIM[Ac]. The CPE-power, n_f for the adsorbed film shows values closer to unity and hence the protective layer which though not truly behaving as a capacitor, does however show more capacitive character than the steel surface. The increase in the capacitive semicircle related to the increase in the values of R'_{ct} indicates increase in inhibition of the corrosion process with increasing concentration of the ILs. Consequently, an increase in inhibition efficiency of the imidazolium-based ILs on the corrosion of carbon steel in the test electrolyte was observed. Comparable values are seen in the inhibition efficiencies *IE* and *IE'* obtained using R_{ct} and R'_{ct} respectively.

3.4. Adsorption and thermodynamic studies

In order to investigate the adsorption characteristics of the employed ILs onto the carbon steel surface, adsorption isotherms were applied. Several of these were utilized to find the best adsorption isotherm describing the adsorption of both EMIM[MS] and EMIM[Ac] on the carbon steel surface in 2 M HCl using data from electrochemical measurements. It was found that the adsorption of both inhibitors obeyed the El-Awardy et al. kinetic-thermodynamic model [27]. This model relates the degree of surface coverage of the inhibitor (θ) to inhibitor's concentration (C) according to Eq. (7);

$$\log\left[\frac{\theta}{1-\theta}\right] = \log K' + y \log C \tag{7}$$

where y is the number of inhibitor molecules occupying one active site (or number of water molecules replaced by one molecule of inhibitor). K' is a constant which is related to the adsorptive equilibrium constant by Eq. (8) [28];

$$K_{ads} = (K')^{1/y} \tag{8}$$

where $1/y = x$, the number of active sites of the surface occupied by one molecule of inhibitor. Large values of K_{ads} mean better

TABLE 4

Electrochemical impedance parameters and the corresponding inhibition efficiencies for API 5L X52 carbon steel in 2 M HCl solution in the absence and presence of different concentrations of inhibitors used at 303 K

Inhibitor system	Inhibitor conc. (M)	R_s (Ω cm^2)	R_f (Ω cm^2)	Q_f (S s^n cm^{-2})	n_f	R_{ct} (Ω cm^2)	Q_{dl} (S s^n cm^{-2})	n_{dl}	*IE* (%)	R'_{ct} (Ω cm^2)	*IE'* (%)
Blank	0	0.1464	8.67	1.307×10^{-4}	0.940	45.37	1.987×10^{-3}	0.622		53.9	
EMIM[MS]	0.001	0.0994	20.32	1.820×10^{-4}	0.890	75.51	0.866×10^{-3}	0.760	40	94.2	43
	0.005	0.1105	21.04	1.713×10^{-4}	0.870	94.39	0.791×10^{-3}	0.785	52	113.3	52
	0.010	0.0847	21.01	1.375×10^{-4}	0.900	97.76	0.771×10^{-3}	0.792	54	116.4	54
EMIM[Ac]	0.001	0.2102	4.650	6.515×10^{-5}	0.988	81.79	1.409×10^{-3}	0.628	44	89.6	40
	0.005	0.2739	10.55	7.001×10^{-5}	0.980	83.71	1.416×10^{-3}	0.619	46	99.0	46
	0.010	0.1219	15.06	7.522×10^{-5}	0.980	91.30	8.743×10^{-4}	0.768	50	104.1	48

inhibition efficiency of a given compound (i.e. stronger electronic interaction for the adsorbing molecule at the surface of the metal). Small values of K_{ads} however indicate weaker interaction by the adsorbing molecules and the metal surface, denoting easy removal of adsorbed molecules by solvent molecules from the metal surface [3].

Fig. 6a and 6b show the El-Awardy isotherm for the adsorption of EMIM[MS] and EMIM[Ac] on carbon steel surface at 303 K and 313 K. Adsorption parameters deduced from the plots are presented in Table 5.

TABLE 5

Adsorption parameters from El -Awardy kinetic-thermodynamic model for the adsorption of EMIM[MS] and EMIM[Ac] in 2 M HCl at 303 K and 313 K

Inhibitor system	Temp (K)	K'	y	x	R^2	K_{ads}	ΔG_{ads} (kJ/mol)
EMIM[MS]	303	10.77	0.48	2.07	0.9706	136.73	–22.51
	313	25.91	0.71	1.42	0.9704	99.99	–22.44
EMIM[Ac]	303	3.31	0.41	2.43	0.8472	18.37	–17.45
	313	3.51	0.46	2.18	0.9079	15.38	–17.57

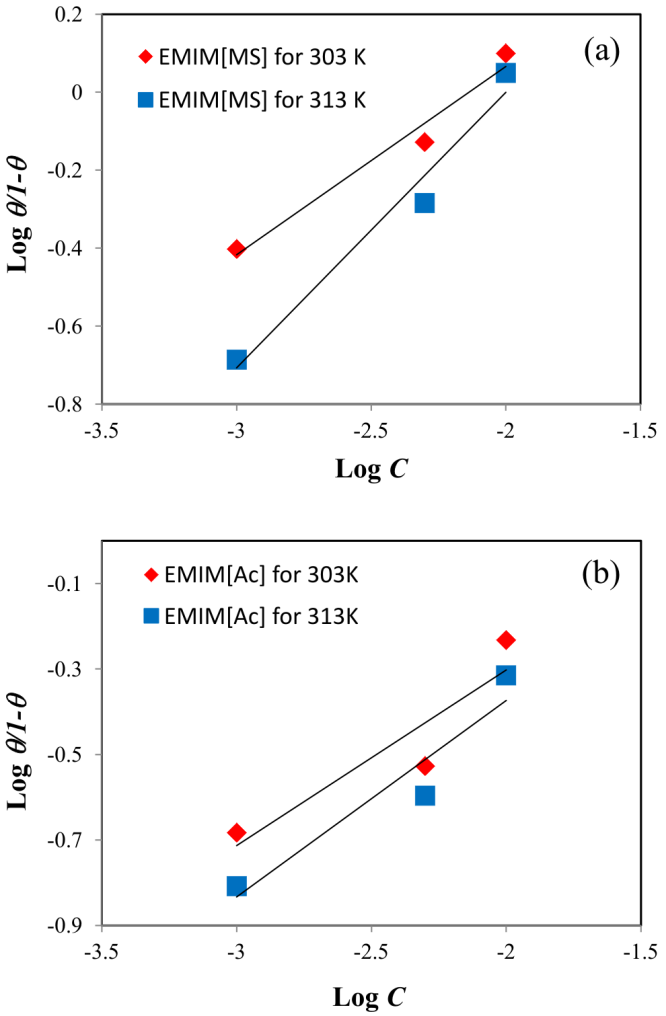

Fig. 6. El-Awardy kinetic-thermodynamic model for the adsorption of (a) EMIM[MS] and (b) EMIM[Ac] on API 5L X52 carbon steel at 303 K and 313 K

Linear plots were obtained which reveal the applicability of this isotherm on the ongoing adsorption process. Values of x were approximately equal for all concentrations of EMIM[MS] and EMIM[Ac]. Therefore, the adsorption of both ILs on carbon steel surface can be regarded as a substitution process, in which an inhibitor molecule in the aqueous phase substitutes an x (in this case, $x \approx 2$) number of water molecules adsorbed on the surface. K_{ads} decreases with increasing temperature suggesting that the inhibitors are physically adsorbed on the metal surface as desorption process enhances with elevating temperature. Furthermore, K_{ads} is related to the adsorption free energy (ΔG^o_{ads}) according to Eq. (9) [29];

$$\Delta G^o_{ads} = -RT \ln\left(55.5 K_{ads}\right) \tag{9}$$

where R is the gas constant (8.314 J K^{-1} mol^{-1}), T is the absolute temperature (K) and 55.5 is the molar concentration of water at the electrode/electrolyte interface in 1 L solution [30]. The calculated ΔG^o_{ads} values for EMIM[MS] ($\approx$ –22 kJ mol^{-1}) whose absolute value is higher than 20 kJ mol^{-1} but sufficiently lower than 40kJ mol^{-1}, indicates that the EMIM[MS] adsorption mechanism on carbon steel surface in 2 M HCl solution was more than an electrostatic adsorption (physisorption), but not a true chemisorption [31,32]. However, for EMIM[Ac], values of ΔG^o_{ads} are found to be $\approx$ –17 kJ mol^{-1} indicating a true physisorption type of adsorption. The negative sign indicates spontaneous interaction of inhibitor molecule with the corroding carbon steel surface.

The activation energies E_a for carbon steel corrosion in 2 M HCl solution in the absence and presence of EMIM[MS] and EMIM[Ac] were evaluated using Arrhenius equation (Eq. (10)) as follows;

$$\ln\left[\frac{CR_1}{CR_2}\right] = \frac{E_a}{R}\left[\frac{1}{T_2} - \frac{1}{T_1}\right] \tag{10}$$

where CR_1 and CR_2 are the corrosion rates at temperatures T_1 and T_2 respectively and R is the gas constant. Estimated values of the heats of adsorption Q_{ads} was obtained from Eq. (11);

$$Q_{ads} = 2.303R\left[\log\left(\frac{\theta_2}{1-\theta_2}\right) - \log\left(\frac{\theta_1}{1-\theta_1}\right)\right] \times \left(\frac{T_1 T_2}{T_2 - T_1}\right) \tag{11}$$

where θ_1 and θ_2 are the degrees of surface coverage at temperature T_1 and T_2 respectively. The activation energy E_a in the inhibited solution (both EMIM[MS] and EMIM[Ac]) is higher than that obtained for the free acid solution (blank) indicating that the corrosion reaction of carbon steel is inhibited by both inhibitors. Since corrosion primarily occurs at surface sites free of adsorbed inhibitor, the higher E_a values in inhibited solutions imply that the ILs screen the active sites on the metal surface thereby decreasing the surface area available for corrosion [33]. It can also be correlated with increasing thickness of the double layer which enhances the E_a of the corrosion process [34] and an indication of a strong inhibitive action of both ILs by increasing energy barrier for the corrosion process, emphasizing

the electrostatic character of the inhibitors' adsorption on the carbon steel surface (physisorption) [35]. The negative value of Q_{ads} indicates that the adsorption of both inhibitors on the carbon steel surface is exothermic. The change in enthalpy of adsorption ΔH_{ads} (Eq. (12)) and change in entropy of adsorption ΔS_{ads} (Eq. (13)) were calculated as follows;

$$\Delta H_{ads} = R\frac{T_1T_2}{T_2 - T_1}\ln\frac{K_2}{K_1} \tag{12}$$

$$\Delta S_{ads} = \frac{\Delta H_{ads} - \Delta G_{ads}}{T} \tag{13}$$

where K_1 and K_2 are the equilibrium adsorption constants at 303 K and 313 K respectively obtained from the slopes of the kinetic-thermodynamic adsorption isotherms. The ΔH_{ads} values for both inhibitors are negative further confirming the exothermic nature of the process. The calculated thermodynamic parameters, E_a, Q_{ads}, ΔG_{ads}, ΔH_{ads} and ΔS_{ads} are presented in Table 6.

3.4. Inhibition mechanism

In order to be able to predict the inhibition mechanism of the adsorption of protonated inhibitor compounds to positively charged Fe surface, we first examine the corrosion mechanism of Fe in HCl in the absence of an inhibitor as proposed by Müller [36] detailing the cathodic hydrogen evolution steps Eq. (14)-Eq. (16):

$$Fe + H^+ \leftrightarrow (FeH^+)_{ads} \tag{14}$$

$$(FeH^+)_{ads} + e^- \rightarrow (FeH)_{ads} \tag{15}$$

$$(FeH)_{ads} + H^+ + e^- \rightarrow Fe + H_2 \tag{16}$$

and anodic dissolution steps Eq. (17)-Eq. (20);

$$Fe + Cl^- \leftrightarrow (FeCl^-)_{ads} \tag{17}$$

$$(FeCl^-)_{ads} \leftrightarrow (FeCl)_{ads} + e^- \tag{18}$$

$$(FeCl)_{ads} \rightarrow \left(FeCl^+\right) + e^- \tag{19}$$

$$FeCl^+ \leftrightarrow Fe^{2+} + Cl^- \tag{20}$$

At cathodic sites on the steel surface, protonated imidazolium molecules are also adsorbed in competition with hydronium ions. Because the IL cations are larger than hydronium ions, the ILs cover a large part of the metallic surface. In the structure of imidazolium bases, the atoms of the imidazolium ring and the –C=N– group can form a big π bond. The π electron of the imidazolium bases enter unoccupied orbitals of Fe in addition to the d-orbital electrons of Fe being accepted by the π^* orbital of the imidazolium bases to form feed-back bonds. The metallic surface is then protected against corrosion as a layer of adsorbed imidazolium molecules is deposited on the steel surface. As electrons are consumed at cathodic sites, the anodic sites are made more positive in potential. Cl^- ions are assumed to be adsorbed onto the positively charged metal surface by coulombic attraction and thereafter the inhibitor molecule can be adsorbed through electrostatic interactions between the positively charged molecules and the negatively charged metal surface [19]. These adsorbed molecules interact with $(FeCl^-)_{ads}$ species to form monomolecular layers by forming a complex on the steel surface, thus protecting the steel surface from attack by Cl^- ions. Hence, the oxidation reaction of $(FeCl^-)_{ads}$ as shown in Eq. (18)-Eq. (20) can be prevented. Meanwhile the presence of the electron donating groups on the imidazolium base structure (O and S), increases the electron density on the nitrogen of the –C≡N– group, resulting in high inhibition efficiency. In particular, S atom is found to have excellent ability to offer free electrons [37].

A proposed mechanism for the corrosion inhibition of the studied compounds detailing the inhibitor reactions at cathodic sites is given in Eq. (21a) for EMIM[MS] and Eq. (21b) for EMIM[Ac].

$$Fe + [EMIM]^+ \leftrightarrow Fe\left[EMIM\right]^+_{ads} + \\ + e^-(MS) \rightarrow Fe\left[EMIM\right][MS]_{ads} \tag{21a}$$

$$Fe + [EMIM]^+ \leftrightarrow Fe\left[EMIM\right]^+_{ads} + \\ + e^-(Ac) \rightarrow Fe\left[EMIM\right][Ac]_{ads} \tag{21b}$$

The reactions of Eq. (21a) and Eq. (21b) slow down the hydrogen evolution process as the protonated imidazolium molecules compete favourably over hydronium ions. The electron donating atoms on the acetate and methanesulphonate species

TABLE 6

Thermodynamic parameters for the inhibition of API 5L X52 carbon steel in 2 M HCl solution containing EMIM[MS] and EMIM[Ac]

Inhibitor system	Inhibitor conc. (M)	E_a (kJ/mol)	Q_{ads} (kJ/mol)	ΔH_{ads} (kJ/mol)	ΔS_{ads} (kJ/mol/K)	
					303 K	313 K
	Blank	7.94				
EMIM[MS]	0.001	19.69	–63.56	–24.67	–0.0071	–0.0071
	0.005	18.94	–28.33			
	0.010	13.10	–9.08			
EMIM[Ac]	0.001	11.32	–100.05	–14.03	0.0113	0.0113
	0.005	10.55	–12.71			
	0.010	13.17	–15.07			

supply electrons to the d-orbitals of Fe forming a layer of adsorbed inhibitor molecules.

At anodic sites, the mechanism is according to Eq. (22);

$$Fe + Cl^- \leftrightarrow (FeCl^-)_{ads} + \\ + [EMIM]^+ \rightarrow (FeCl^-[EMIM]^+)_{ads} \quad (22)$$

Cl^{-1} ions are specifically adsorbed to the surface of steel as the surface charge of steel is known to be positive in HCl solution [38]. The $(FeCl^-)_{ads}$ species formed favours the adsorption of the protonated inhibitor molecules by electrostatic attraction. The anodic dissolution process is hence retarded as the adsorbed inhibitor molecules form a protective layer on the steel surface. The adsorption of the inhibitor molecules reduces any further action of the aggressive Cl^- ions. These equations reflect the mixed type inhibitor behaviour earlier deduced. Also, a larger molecular size leads to larger surface coverage thereby enhancing inhibition performance [39]. EMIM[MS] has a molecular weight of 206.26 g mol^{-1} and is greater in weight than EMIM[Ac] of 170.21 g mol^{-1}. The effectiveness of EMIM[MS] in inhibiting the corrosion of carbon steel in HCl over EMIM[Ac] can be attributed its larger molecular size and weight which is related to the surface coverage, steric effect and the presence of the electron donating sulphur atom that increases the electron density at donor sites.

4. Conclusion

The effect of two ionic liquids, EMIM[MS] and EMIM[Ac] on the corrosion inhibition of API 5L X52 carbon steel in 2 M HCl solution was studied using gravimetric and electrochemical methods. The results showed EMIM[MS] having better inhibiting efficiency than EMIM[Ac] with inhibition efficiency increasing with increasing inhibitor concentration. The application of EMIM[MS] and EMIM[Ac] inhibitors significantly increases R_{ct} values indicative of a reduction in corrosion rate. The values of K_{ads} obtained for EMIM[MS] was higher than that obtained for EMIM[Ac] indicating that EMIM[MS] is more strongly adsorbed on API 5L X52 carbon steel surface and has a better inhibition efficiency. The inhibition efficiency was found to decrease with increase in temperature suggesting a physical adsorption mechanism. The increase in activation energy on the addition of inhibitors to the 2 M HCl solution and the value of the free energy of adsorption indicated that the adsorption is more physical than chemical. EMIM[MS] was found to be a more effective corrosion inhibitor because of the presence of oxygen and sulphur atoms in the imidazolium base structure and its higher molecular weight compared to EMIM[Ac].

Acknowledgement

This work was supported by China-Africa Science and Technology Partnership Program (CASTEP).

REFERENCES

[1] K.O. Abiola, N.C. Oforka, E.E. Ebenso, N.M. Nwinuka, Anti-Corros. Method M. **54** (4), 219-224 (2007).
[2] M. Abdallah, Corros. Sci. **46** (8), 1981-1986 (2004).
[3] N.O. Eddy, E.E. Ebenso, Pigm. Resin Technol. **39** (2) 77-84 (2010).
[4] E.E. Ebenso, H. Alemu, S.A. Umoren, I.B. Obot, Int. J. Electrochem. Sci. **3**, 1325-1331 (2008).
[5] R.D. Rogers, K.R. Seddon, Science. **302**, 792-797 (2003).
[6] J.S. Wilkes, Green Chemistry. 4, 73-82 (2002).
[7] S.A. Forsyth, J.M. Pringle, D.R. MacFarlane, Aust. J. Chem. **57**, 113-1120 (2004).
[8] A.F. Al-Ghamdi, M. Messali, S.A. Ahmed, J. Mater. Environ. Sci. **2**, 215-224 (2011).
[9] H.L. Ngo, K. LeCompte, L. Hargens, A.B. McEwen, Thermochim. Acta. **97**, 357-358 (2000).
[10] F. Endres, S.Z. El Abedin, S. Matter, Phys. Chem. Chem. Phys. **8** (18), 2101-2116 (2006).
[11] M.A.M. Ibrahim, M. Messali, Z. Moussa, A.Y. Alzahrani, S.N. Alamry, B. Hammouti, Port. Electrochim. Acta, **29** (6), 375-389 (2011).
[12] C. Jungnickel, J. Łuczak, J. Ranke, J.F. Fernández, A. Müller, J. Thöming, Colloid Surface A Physicochem. Eng. Asp. **316**, 278-284 (2008).
[13] E.A. Noor, A.H. Al-Moubaraki, Int. J. Electrochem. Sci. **3**, 806-818 (2008).
[14] D.Q. Zhang, L.X. Gao, G.D. Zhou, Appl. Surf. Sci. **252**, 4975-4981 (2006).
[15] M. Messali, J. Mat. Environ. Sci. **2**, 174-179 (2011).
[16] M. Corrales-Luna, T.L. Manh, M. Romero-Romo, M. Palomar-Pardave, E. M. Arce-Estrada, Corros. Sci. **153**, 85-99 (2019).
[17] A. Zarrouk, M. Messali, H. Zarrok, R. Salghi, A.A. Al-Sheikh, B. Hammouti, S.S. Al-Deyab, F. Bentiss, Int. J. Electrochem. Sci. **7**, 6998-7015 (2012).
[18] Q.B. Zhang, Y.X. Hua, Electrochim. Acta. **54**, 1881-1892 (2009).
[19] M.A. Quraishi, M.Z.A. Rafiquee, K. Khan, N. Saxena, J. Appl. Electrochem. **37**, 1153-1162 (2007).
[20] Q. Zhang, Y. Hua, Mater. Chem. Phys. **119**, 57-64 (2010).
[21] M.E. Ikpi, F.E. Abeng, Int. J. Sci. Res. **6** (6) 623-628 (2017).
[22] P.A.L. Anawe, C.U. Obi, S.S. Mehdi, K.O. Ogunniran, B.I. Ita, C.O. Ehi-Eromosele, Prot. Met. Phys. Chem. S. **51** (3), 458-466 (2015).
[23] S. Rajendran, M. Reenkala, N. Anthony, R. Ramaraj, Corros. Sci. **44**, 2243-2252 (2002).
[24] C. Cao, Corros. Sci. **38**, 2073-2082 (1996).
[25] S. Nesic, Corros. Sci. **49**, 4308-4338 (2007).
[26] R.F.A. Jargelus-Pettersson, B.G. Pound. J. Electrochem. Soc. **145**, 1462-1469 (1998).
[27] A.A. El-Awardy, B.A. Abd-El-Nabey, S.G. Aziz, J. Electrochem. Soc. **139**, 2149-2154 (1992).
[28] A. Khadom, A.S. Yaro, A.S. AlTaie, A.A. H. Kadhum, Port. Electrochim. Acta. **27** (6), 699-712 (2009).
[29] A. Ghanbari, M.M. Attar, M. Mahdavian, Mater. Chem. Phys. **124**, 1205-1209 (2010).

[30] S.T. Arab, A.M. Turkustuni, Port. Electrochim. Acta. **24**, 53-69 (2006).
[31] G. Moretti, F. Guidi, G. Grion, Corros. Sci. **46**, 387-403 (2004).
[32] R. Solmaz, Corros. Sci. **79**, 169-176 (2014).
[33] H.M. Bhajiwala, R.T. Vashi, B. Electrochem. **17** (10), 441-448 (2001).
[34] M.M. Solomon, S.A. Umoren, I.I. Udosoro, A.P. Udoh, Corros. Sci. **52** (4) 1317-1325 (2010).
[35] S.A. Umoren, I.B. Obot, E.E. Ebenso, N.O. Obi-Egbedi, Port. Electrochim. Acta. **26**, 199-209 (2008).
[36] M. Müller, Inorganic Structure Chemistry, John Wiley & Sons, New York (2006).
[37] J. Fang, J. Li, J. Mol Struct-Theochem. **593**, 179-185 (2002).
[38] S. Deng, X. Li, Corros. Sci. **55**, 407-415 (2012).
[39] L.L. Liao, S. Mo, H.Q. Luo, Y.J. Feng, H.Y. Yin, N.B. Li, Corros. Sci. **124**, 167-177 (2017).